A COOH-terminal peptide confers regiospecific orientation and facilitates atomic force microscopy of an IgG_1

C. R. Ill,* V. M. Keivens,* J. E. Hale,* K. K. Nakamura,‡§ R. A. Jue,* S. Cheng,* E. D. Melcher,* B. Drake,§ and M. C. Smith‖

*Protein Engineering Group, Division of Imaging and Therapeutic Research, Hybritech, Inc., San Diego, California 92121; ‡Protein Chemistry Division, Ixsys Inc., San Diego, California 92121; §Imaging Services Inc., Santa Barbara, California 93111; and ‖Virology Research Laboratory, Lilly Research Laboratories, Eli Lilly and Company, Indianapolis, Indiana 46285 USA

ABSTRACT An antibody (IgG_1) was designed for oriented adherence to a metal-containing surface. This was achieved by adding a metal-chelating peptide, (CP = His-Trp-His-His-His-Pro), to the COOH-terminus of the heavy chain through genetic engineering. Electroporation of the engineered heavy chain gene into cells expressing the complimentary light chain yielded colonies secreting an intact antibody containing the metal-chelating peptide (IgG_1-CP) which had high affinity for a nickel-loaded iminodiacetate column. Purified IgG_1-CP was bound to nickel-treated mica and imaged by atomic force microscopy (AFM). Antibody lacking the COOH-terminal metal binding peptide failed to produce discernible AFM images. The AFM images of individual IgG_1-CP molecules and their calculated dimensions demonstrated that regiospecific binding and uniform orientation of the antibody was imparted by the peptide. The ability to stably orient macromolecules in their native state to a surface may be used advantageously to visualize them.

INTRODUCTION

Atomic Force Microscopy (AFM) is a highly useful tool for visualizing the three-dimensional structures of proteins and polynucleotides. AFM and similar atomic-scale visualization instruments, such as the Scanning Tunneling Microscope (STM), are serving as prototypes for the development of tools to not only visualize, but eventually to manipulate individual molecules and atoms (1).

In order to utilize these instruments, it is necessary to immobilize the molecules to be visualized or manipulated so that the mechanical forces involved in the procedure do not physically remove the molecules from the surface of the AFM substrate. Attachment of molecules to a substrate for observation or manipulation under native conditions has proven difficult. For example, to image plasmid DNA, Hansma et al. (2) found it necessary to alcohol-precipitate the DNA onto the AFM substrate, to prevent its movement by the AFM cantilever tip. Similarly, Lin et al. (3), described the imaging of IgG molecules by AFM, but they could not achieve adherence of the proteins to the surface without forming "lateral interactions" among the molecules. As a result, a random latticework of IgG molecules formed and individual protein molecules were desorbed from the AFM substrate. Weisenhorn et al. (4), were able to image immunoglobulin Fab' fragments by covalently linking Fab' molecules to a lipid and incorporating them into a lipid monolayer on the AFM substrate. Although imaging was done under native conditions, extensive preparation of the AFM surface was required, as well as chemical modification of the Fab'. Furthermore, increases of the applied force to above 10 nN pushed aside the proteins, exposing only the lipid membrane.

Address correspondence to Dr. Charles R. Ill, Protein Engineering Group, Division of Imaging and Therapeutic Research, Hybritech, Inc., 11095 Torreyana Road, San Diego, CA 92121, USA.

We describe here a means of anchoring protein molecules for observation in AFM under native conditions which employs a metal-chelating peptide. No labor-intensive preparation of the AFM surface or chemical modification of the protein is required. Addition of the metal-chelating peptide to the IgG COOH-terminus allows the COOH-terminal region of the protein to be anchored to the nickel–mica AFM substrate. As a result, uniform orientation is achieved and the particular region of interest can be visualized. Furthermore, unlike chemical modification, genetic engineering allows the specific placement of the anchoring peptide to any desired position on the molecule, so that other regions of interest can be visualized. Orientation of molecules under native conditions will also maximize the binding of a second molecular species to a specific location on the anchored species (5).

MATERIALS AND METHODS

Construction of IgG_1-CP

Construction of the complete expression vector involved generating four DNA fragments from a previously described gamma-1 expression vector called $pNCEMG_1$ (6). The first 9.0 kilobase fragment was generated using restriction enzymes Nru-1 and Sal-1 (GIBCO BRL, Gaithersburg, MD) and contained the neomycin, beta-lactamase and heavy chain variable region gene sequences. The second 1.8 kilobase fragment was generated by PCR-amplifying (PCR kit was obtained from Perkin Elmer Cetus, Norwalk, CT) the region of $pNCEMG_1$ containing the constant region gene using an upstream primer that contained 30 base pairs of sense strand sequence 5' of the Sal-1 site, and a downstream primer that contained 30 base pairs of the antisense strand, the sequence coding for His-Trp-His-His-His-Pro, a stop codon, and Xma-III site at its 5' end. Once amplified, this fragment was cloned into pBR322 for confirmation of the desired nucleotide sequence. The third 324 base pair fragment was generated using an upstream primer that contained at its 5' end the metal binding peptide sequence, stop codon, Xma-III site, 30 base pairs of sense strand sequence, and a downstream primer that contained 30 base pairs of antisense sequence and the restriction site sequence for Nru-1 at its 5' end. This fragment was needed

0006-3495/93/03/919/06 $2.00

to include the polyadenylation sequence and to overlap with the metal binding peptide sequence in fragment 2. Overlapping or recombinant PCR (7) was carried out for the generation of the final 2.1 kilobase fragment. Fragment 4 was subcloned into a TA cloning vector (In Vitrogen Corp., San Diego, CA) which contains single 3′ deoxythymidylate overhangs and takes advantage of the terminal transferase activity of thermophilic DNA polymerase, which adds a single 3′ deoxyadenylate residue to each end of the amplified fragment. Fr-4 was isolated from the TA vector by a Sal-1/Nru-1 restriction enzyme digest and ligated together with Fr-1 to generate the 11.2 kilobase pNCEMG$_1$-CP.

PURIFICATION OF IgG$_1$-CP FROM CHEL-13 SUPERNATANT

Concentrated culture supernatant from terminal cultures of CHEL-13 secreting cells grown in serum free media was dialyzed against Buffer A (100 mM NaH_2PO_4, pH 7.4; 100 mM NaCl) at 4°C for 18 h. Following dialysis the media was centrifuged at 3000 *g* for 10 min. The clarified media was decanted and filtered through a 0.2 μm filter. A 2.1 × 30 mm iminodiacetate HPLC column from Perspective Biosystems was loaded with Ni^{2+} according to the manufacturer's instructions. The Ni^{2+} loaded column was equilibrated with Buffer A on a Hewlett-Packard 1090 HPLC. Clarified media (5.0 ml) was injected onto the column at a flow rate of 1.0 ml/min. After the media was loaded, the column was washed with 5.0 ml of Buffer A. The column was washed successively with 5 ml 50% Buffer A; 50% Buffer B (100 mM NaH_2PO_4, pH 4.25; 100 mM NaCl) then with 5.0 ml Buffer B. Following these washes the column was re-equilibrated with 1.0 ml Buffer A. Bound CHEL-13 was eluted with a linear gradient from Buffer A to Buffer C (1 M glycine, pH 8.7; 100 mM NaCl) developed over 10 min. Fractions (1 min.) were collected and analyzed for antibody content by SDS-PAGE (8). Residual bound nickel was removed from the IgG$_1$-CP by treatment with 10 mM EDTA in PBS. The EDTA was removed from the antibody solution by concentrating the antibody in an Amicon cell with a YM-10 membrane. The antibody was diluted in EDTA-free PBS. This cycle of concentration and dilution was repeated until the EDTA was diluted by a factor of 10^5.

ATOMIC FORCE MICROSCOPY OF IgG$_1$ AND IgG$_1$-CP

Nickel-coated mica with IgG$_1$ and with IgG$_1$-CP were imaged in a fluid cell containing PBS (10 mM NaH_2PO_4, pH 7.0, 150 mM NaCl) at room temperature. All images were obtained using a NanoScope II atomic force microscope (Digital Instruments, Santa Barbara, CA) (9) with a 12 μm Scanner and a 120 μm Si_3N_4 cantilever (K = 0.6 N/m). Two-dimensional top views and 3-D views are 300 by 300 nm scale. The freshly-cleaved mica surface was treated with 5 ml of 1 mM nickel-chloride dissolved in MilliQ water for 1 min, rinsed three times with 1 ml of MilliQ water, and allowed to air dry. The IgG$_1$ or IgG$_1$-CP were diluted to a concentration of 0.5 μg/ml in PBS, injected into the fluid cell, and allowed to interact with the nickel–mica surface for 10 min. The fluid cell was then flushed with PBS and the images were collected. The molecular dimensions were taken directly from the best multiple images of individual molecules. The measurements are approximate average dimensions of the diameter of the globular shaped antibodies. The heights are average maximum thicknesses.

RESULTS AND DISCUSSION

In designing an IgG$_1$ with an added metal binding sequence it was necessary to modify the sequence in such a way as to prevent disturbances to the functional and structural portions of the native molecule. Inspection of the human IgG$_1$ Fc crystal structure (10) revealed an approximate 21 Å distance between the COOH-terminal residues of the two heavy chains.[1] The addition of the metal binding sequence was thus not expected to interfere with association of the heavy chains of the H_2L_2 IgG$_1$-CP. A His-Trp-His-His-His- sequence was chosen for its ability to bind tightly to a nickel or cobalt-loaded metal affinity column (11). A proline was added to the COOH-terminus to inhibit any potential processing of the antibody by carboxypeptidases. For rapid site-directed mutagenesis of the IgG$_1$ heavy chain gene the cloning restriction sites and the 18 base pair metal binding peptide sequence were engineered into the primers of three separate polymerase chain reactions (Fig. 1 *A* and *B*). Overlapping or recombinant PCR (7) was carried out for the generation of the final 2.1 kilobase fragment (Fig. 1 *B*).

The pNCEMG$_1$-CP heavy chain expression vector was transfected by standard electroporation conditions for mammalian cell gene expression (12–14) with modifications to obtain the highest secreting clone (15). The clone selected for the highest expression of intact antibody-CP (called chel-13) expressed the complimentary kappa light chain in excess of the intact antibody, i.e., 30 μg/10^6 cells of kappa light chain and 2.7 μg/10^6 cells of intact antibody.

Supernatant containing IgG$_1$-CP from high density chel-13 cultures grown in a serum-free medium formulation (16) was purified by metal affinity HPLC yielding the 4-peak chromatogram shown in Fig. 2. Fractions from the peaks were analyzed by SDS-PAGE (Fig. 2 *inset*) and the proteins were identified as immunoglobulin by western blotting with anti–human heavy chain and anti–human light chain reagents (data not shown). Some free kappa chain and kappa dimer was seen to bind to the column. These chains eluted from the column at pH5.8 and pH4.25, respectively, and appear as 25 and 50 kD bands in the gel. The binding of these chains was not quantitative as evidenced by the large amount of free kappa and kappa dimer in the flow-through fraction, suggesting that the binding is due to endogenous His containing sequences that may not be sterically accessible in all cases. IgG$_1$-CP was eluted with a glycine gradient. Glycine is known to strip the nickel off of the column and the need for glycine to elute IgG$_1$-CP suggests that its affinity for nickel is relatively high. IgG$_1$ without a COOH-terminal chelating peptide binds weakly to the IMAC column (data not shown) presumably through endogenous surface exposed histidines. Its elution at pH 4.25 and inability to bind to nickel-coated mica for atomic force microscopy (see below) suggested lower affinity of the endogenous sequence. While the absolute affinities of the unmodified IgG$_1$ versus the

[1] The molecular modeling system was from Silicon Graphics (Palo Alto, CA) using Insight II software from Biosym (San Diego, CA).

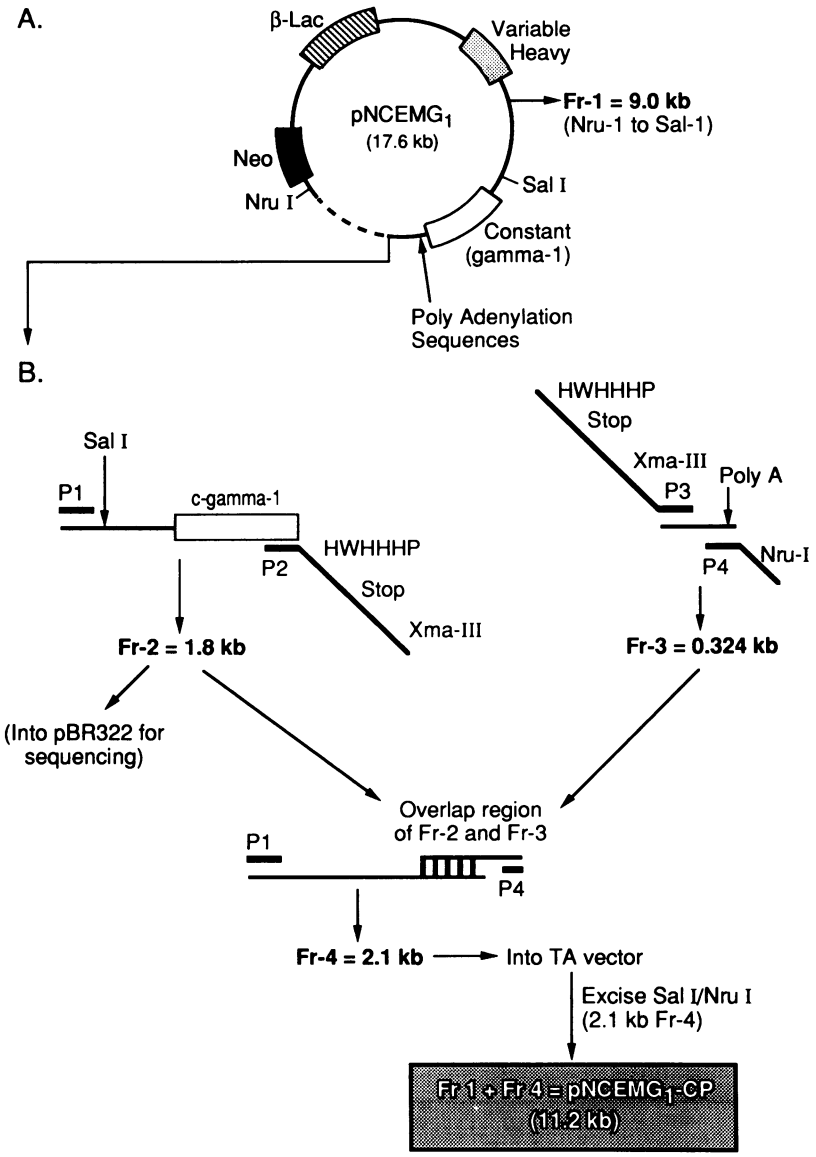

FIGURE 1 *Cloning Scheme for pNCEMG$_1$-CP:* (*A*) The construction of the 17.6 kilobase chimeric expression vector pNCEMG1 has been described (6). Briefly, the expression vector contains the murine variable region of an anti-CEA murine heavy chain gene and the constant region from a human IgG$_1$ gene. The neomycin and beta-lactimase genes are for mammalian and bacterial drug selection, respectively. A 9.0 kilobase fragment 1 (Fr-1) containing all but the human constant region gene was isolated from an Nru-1 to Sal-1 restriction enzyme digest without further modification. The area of the vector marked with cross-hatches indicates approximately 5.5 kilobases of the 3′ untranslated human gamma-1 gene sequence which was deleted as a result of the construction of pNCEMG1-CP. (*B*) Three modified fragments, Fr-2, Fr-3, and Fr-4, were generated from pNCEMG1 (substrate) by the polymerase chain reaction as described in Materials and Methods. All site-directed mutations were achieved by specific sequence addition to the 5′ end of the primers. Fr-2 and the final 11.2 kilobase pNCEMG1-CP expression vector were confirmed to have the desired His-Trp-His-His-His-Pro modification by DNA sequencing and PCR using a primer specific for this sequence addition.

IgG$_1$-CP for nickel have not been determined, other studies have shown that elution profile and partition coefficients can be directly correlated with strength of the protein–metal interaction (17–19). We further demonstrate the strength of the protein-metal interaction by direct visualization of the IgG$_1$-CP in a fluid cell by atomic force microscopy.

Freshly cleaved mica produces a surface well-suited for high resolution microscopy. It is known, however, that proteins do not adhere well to mica and that anchoring proteins to withstand the force of the atomic force microscope stylus is a major hurdle for high resolution imaging (3, 20, 21). Fig. 3 shows that by using the His-Trp-His-His-His-Pro metal-binding sequence engineered into the carboxy terminus of the antibody combined with nickel treatment of the mica surface, stable adherence and orientation of the IgG$_1$ was possible. Figure 3 *a* and 3 *d* are two images of freshly cleaved mica coated with nickel chloride. Two dimensional Fourier transform analysis of atomic scale images (data not

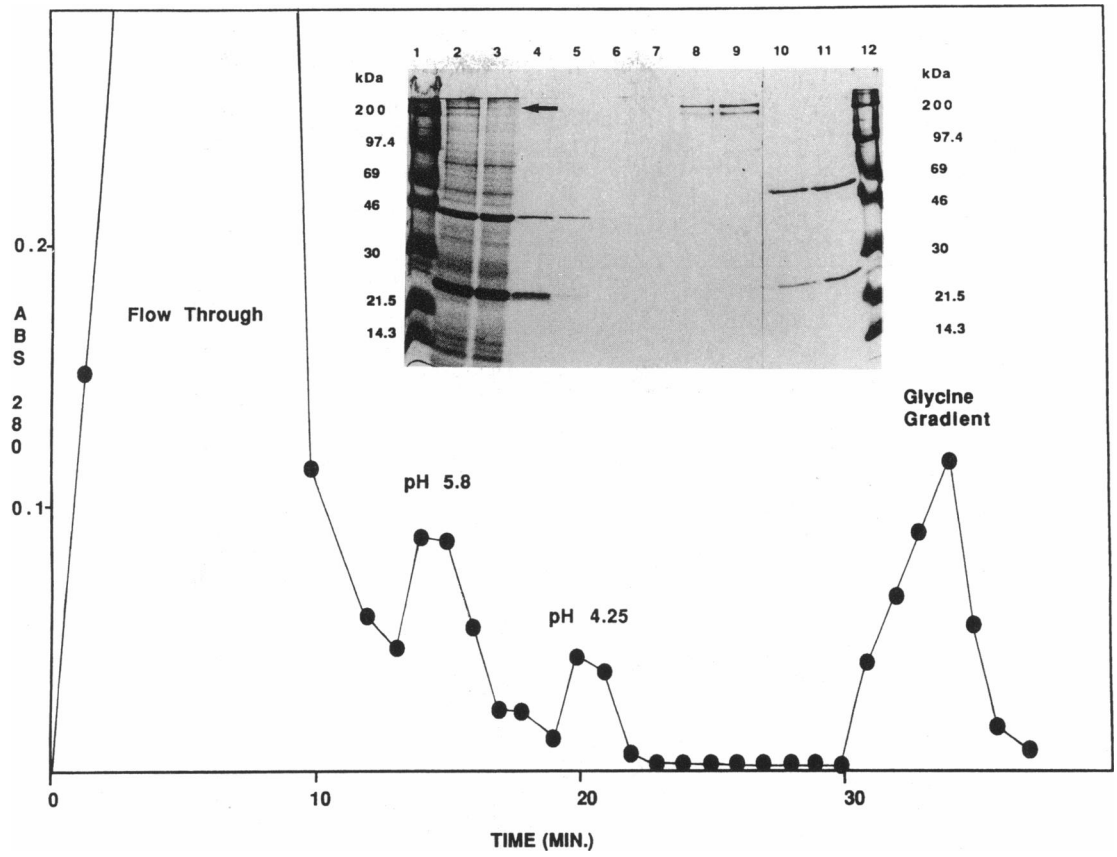

FIGURE 2 *Purification of IgG_1-CP from Chel-13 Supernatant:* Chel-13 containing cell culture media was processed and loaded onto a nickel-loaded iminodiacetate column and bound proteins were eluted as described in Materials and Methods. The peaks are labeled with the buffer conditions under which they eluted. The glycine gradient was begun at 28 min. *Inset: SDS-PAGE Analysis of Fractions from the Iminodiacetate Column:* Aliquots of the CHEL-13 containing media and fractions from the iminodiacetate column were separated on a 12% SDS-PAGE gel (8). Lanes 1–9 & 12; non-reducing, lanes 10 & 11; reducing. Lanes 1 & 12 high MW standards, lane 2; 40 μg CHEL-13 media, lane 3; 40 μg column flow through fraction 4, lane 4; 3 μg fraction 13, lane 5; 2 μg fraction 20, lane 6; 2 μg fraction 31, lane 7; 2.5 μg fraction 32, lane 8; 3.5 μg fraction 33, lane 9; 4.5 μg fraction 34, lane 10; 3.5 μg fraction 33, lane 11; 4.5 μg fraction 34. The arrow in lane 4 shows the absence of antibody in lane 3.

shown) of nickel-coated mica showed hexagonal symmetry plus high frequency peaks confirming nickel-binding, ie., these were not present in mica alone. Fig. 3 *b* and 3 *e* are images of the unmodified IgG_1 preincubated with the nickel-coated mica at a concentration of 0.5 μg/ml. The force applied by the silicon nitride cantilever was approximately 10^{-9}–10^{-10} Newtons. The pressure beneath the tip is estimated to be $\sim 10^7$–10^9 Pascal. The large uncertainty in the applied force is in part caused by the variability of the cantilever spring constant. The obvious smearing of the protein by the cantilever suggests that the antibody is not tightly bound to this surface. Fig. 3 *c* and 3 *f* are images of the IgG_1-CP preincubated on the nickel-coated mica surface at a similar concentration and in an identical manner as those in Fig. 3 *b* and 3 *e*. All images are 300 by 300 nm areas. The globular structures imaged in Fig. 3 *c* and 3 *f* were not displaced by the cantilever using identical applied forces. (Applied forces as high as 10^{-7} N were used with no apparent damage to the IgG_1-CP. Prolonged imaging (10 min), however, and therefore prolonged forces, eventually scraped away the antibody from the AFM substrate). Size determination showed them to be 14.0 nm in diameter by 3.4 nm tall, which corresponds closely to IgG_1 dimensions determined by electron microscopic measurements and x-ray diffraction (22, 23). Preincubation of the IgG_1-CP with a concentrated nickel chloride solution prevented tight binding to the nickel-coated mica surface. In addition, IgG_1-CP did not bind tightly to mica that was not coated with nickel chloride. The stability of the molecules relative to cantilever force, molecular dimensions, homogeneous appearance, and dependence on the interaction of the metal binding sequence with nickel-coated mica, all demonstrate the regiospecific orientation of the IgG_1-CP to this metal-bound surface.

CONCLUDING REMARKS

We have shown that an antibody molecule possessing an engineered metal chelating peptide will bind to a metal ion immobilized on an AFM substrate in a manner sufficiently stable to resist the disrupting forces encountered

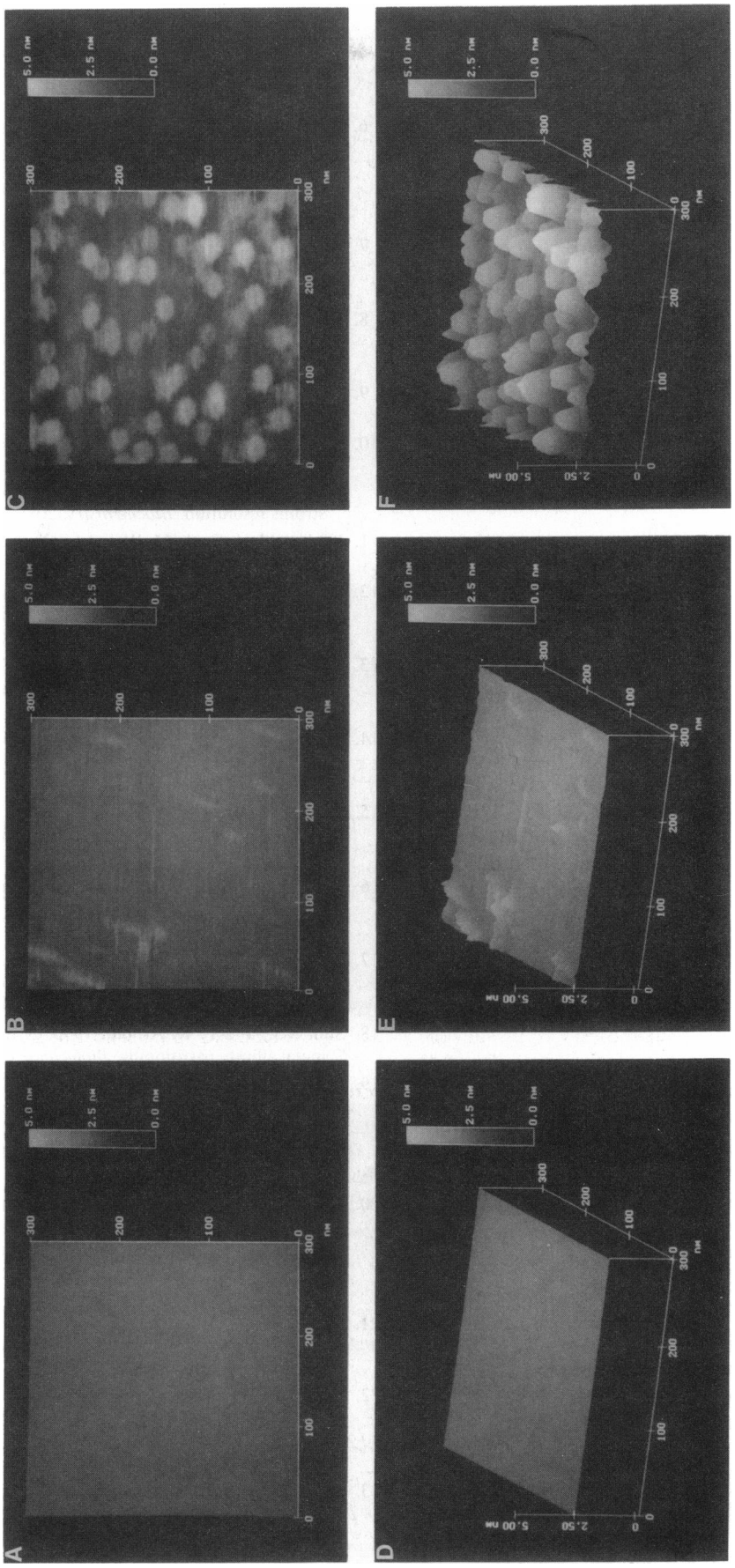

FIGURE 3 *Atomic Force Microscopy of IgG_1 and IgG_1-CP:* Nickel-coated mica (3a,d), with IgG_1 (3b,e) and with IgG_1-CP (3c, f) were imaged in a fluid cell containing PBS as described in Materials and Methods. Two-dimensional top views (3a–c) and 3-D views (3d–f) are shown at a 300 nm by 300 nm scale.

during interaction with a mechanical entity such as an AFM tip. By engineering the chelating peptide onto the COOH-terminus of the antibody we were able to anchor the antibody to the AFM substrate by a specific region of the molecule, ensuring uniform orientation of the bound antibody molecules. The binding of antibody to substrate occurred under buffer conditions compatible with the native conformation of the protein.

That the antibody image did not appear to be "Y" or "T" shaped as one might expect may be explained by the relatively blunt AFM tip. The silicon nitride cantilevers have a gross tip radius of approximately 50 nm, however the "roughness" of the tip is unknown and no one has yet been able to measure the lowest point of the tip, which is thought to be the effective tip. In future studies it will be of interest to try oxide sharpened Si_3N_4 tips or "super tips" (2). It is also a possibility that in the PBS solution, the antibody would not adopt a rigid conformation that would be required in order for the characteristic "Y" or "T" shape to be seen.

Anchoring the antibody by its COOH-terminus should maximize the exposure of the combining site (which is comprised of the NH_2-terminal portion of the protein) as has been observed to occur in antibody affinity columns (5). Additionally, by anchoring the protein under non-denaturing conditions it should retain its biological activity. Anchored, oriented, active antibody should provide a system well suited for the examination of real-time antigen–antibody interactions by direct visualization by AFM. Future developments in this area should strengthen AFM as a technique complimentary to the other biochemical and biophysical techniques currently used to examine protein structure and function.

Received for publication 14 September 1992 and in final form 31 October 1992.

REFERENCES

1. Hansma, P. K., V. B. Elings, O. Marti, and C. E. Bracker. 1988. Scanning tunneling microscopy and atomic force microscopy: Application to biology and technology. *Science (Wash. DC).* 242:209–216.
2. Hansma, H. G., J. Vesenka, C. Siegerist, G. Kelderman, H. Morrett, R. L. Sinsheimer, V. Elings, C. Bustamante, and P. K. Hansma. 1992. Reproducible imaging and dissection of plasmid DNA under liquid with the atomic force microscope. *Science (Wash. DC).* 256:1180–1184.
3. Lin, J. N., B. Drake, A. S. Lea, P. K. Hansma, and J. D. Andrade. 1990. Direct observation of immunoglobulin adsorption dynamics using the atomic force microscope. *Langmuir.* 6:509–511.
4. Weisenhorn, A. L., B. Drake, C. B. Prater, S. A. C. Gould, P. K. Hansma, F. Ohnesorge, M. Egger, S. P. Heyn, and H. E. Gaub. 1990. Immobilized proteins in buffer imaged at molecular resolution by atomic force microscopy. *Biophysical Journal.* 58:1251–1258.
5. Loetscher, P., L. Mottlau, and E. Hochuli. 1992. Immobilization of monoclonal antibodies for affinity chromatography using a chelating peptide. *J. Chrom.* 595:113–119.
6. Beidler, C. B., J. R. Ludwig, J. Cardenas, J. Phelps, C. G. Papworth, E. Melcher, M. Sierzega, L. J. Myers, B. W. Unger, M. Fisher, G. S. David, and M. J. Johnson. 1988. Cloning and high level expression of a chimeric antibody with specificity for human carcinoembryonic antigen. *J. Immunol.* 141:4053–4060.
7. Higuchi, R. 1989. Using PCR to engineer DNA. *In* PCR Technology: Principles and Applications for DNA Amplification. H. A. Erlich, editor, Stockton Press, New York, 61–70.
8. Jue, R. A., and R. F. Doolittle. 1985. Determination of the relative positions of amino acids by partial specific cleavages of end-labeled proteins. *Biochemistry.* 24:162–169.
9. NanoScope II Handbook. Digital Instruments, Santa Barbara, CA. 93117.
10. Deisenhofer, J. 1981. Crystallographic refinement and atomic models of a human Fc fragment and its complex with fragment B of protein A from *Staphylococcus aureus* at 2.9- and 2.8 Angstroms resolution. *Biochemistry.* 20:2361–2378.
11. Kasher, M., J. Cook, M. Wakulchik, and M. C. Smith. 1992. Biotechniques. (In press).
12. Toneguzzo, F., A. Hayday, and A. Keating. Electric field-mediated DNA transfer: Transient and stable gene expression in human and mouse lymphoid cells. 1986. *Mol. Cell. Biol.* 6:703–706.
13. Chu, G., H. Hayakawa, and P. Berg. 1987. Electroporation for the efficient transfection of mammalian cells with DNA. *Nucl. Acids Res.* 15:1311–1326.
14. Andreason, G., and G. Evans. 1988. Introduction and expression of DNA molecules in eukaryotic cells by electroporation. *Biotechniques.* 6:650–659.
15. Condon, T. P., J. E. N. Gonzales, and C. R. Ill. 1991. Different electric field strengths for maximum efficiency or expression in electroporation. *Focus.* 13:33–35.
16. Ill, C. R., T. Brehm, B. J. Lydersen, R. Hernandez, and K. Burnett. 1988. Species specificity of iron delivery in hybridomas. *In Vitro Cell. Devel. Bio.* 24:413–419.
17. Smith, M. C., T. C. Furman, T. D. Ingolia, and C. Pidgeon. 1988. Chelating peptide-immobilized metal ion affinity chromatography. *J. Biol. Chem.* 263:7211–7215.
18. Suh, S-S., and F. R. Arnold. 1990. A mathematical model for metal affinity partitioning. *Biotechnol. and Bioeng.* 35:682–696.
19. Hutchens, T. W., T-T. Yip, and J. Porath. Protein interaction with immobilized ligands: Quantitative analyses of equilibrium partition data and comparison with analytical chromatographic approaches using immobilized metal affinity adsorbents. 1988. *Anal. Biochem.* 170:168–182.
20. Drake, B., C. B. Prater, A. L. Weisenhorn, S. A. C. Gould, T. R. Albrecht, C. F. Quate, D. S. Cannell, H. G. Hansma, and P. K. Hansma. 1989. Imaging crystals, polymers, and processes in water with the atomic force microscope. *Science (Wash. DC).* 243:1586–1589.
21. Heuser, J. 1989. Protocol for 3-D visualization of molecules on mica via the quick-freeze, deep-etch technique. *J. Elec. Micr. Tech.* 13:244–263.
22. Eisen, H. N. Immunology. 1974. Harper & Row, New York. 289 pp; co-printed in Microbiology. 2nd Ed. B. D. Davis, R. Dulbecco, H. N. Eisen, H. S. Ginsberg, and W. B. Wood, editors. Harper & Row.
23. Sarma, V. R., E. W. Silverton, D. R. Davies, and W. D. Terry. 1971. *J. Biol. Chem.* 246:3753–3759.